IEICE TRANS. ELECTRON., VOL.E104–C, NO.6 JUNE 2021

BRIEF PAPER *Special Section on Recent Progress in Organic Molecular Electronics*

Fabrication of Silicon Nanowires by Metal-Catalyzed Electroless Etching Method and Their Application in Solar Cell

Naraphorn TUNGHATHAITHIP[†,††], **Chutiparn LERTVACHIRAPAIBOON**[†], ***Nonmembers***, **Kazunari SHINBO**[†], ***Member***, **Keizo KATO**[†], ***Fellow***, **Sukkaneste TUNGASMITA**[††a)], ***Nonmember***, ***and*** **Akira BABA**[†b)], ***Member***

SUMMARY We fabricated silicon nanowires (SiNWs) using a metal-catalyzed electroless etching method, which is known to be a low-cost and simple technique. The SiNW arrays with a length of 540 nm were used as a substrate of SiNWs/PEDOT:PSS hybrid solar cell. Furthermore, gold nanoparticles (AuNPs) were used to improve the light absorption of the device due to localized surface plasmon excitation. The results show that the short-circuit current density and the power conversion efficiency increased from 22.1 mA/cm^2 to 26.0 mA/cm^2 and 6.91% to 8.56%, respectively. The advantage of a higher interface area between the organic and inorganic semiconductors was established by using SiNW arrays and higher absorption light incorporated with AuNPs for improving the performance of the developed solar cell.

key words: *SiNWs, MCEE method, hybrid solar cell, PEDOT:PSS, AuNPs*

1. Introduction

Silicon nanowires (SiNWs) are considered as one of the most important and popular nanostructural substrates for many applications because of their unique electrical and optical properties that are not present in bulk structures [1], [2]. Several techniques on the fabrication of SiNWs have been proposed, such as vapor-liquid-solid growth [3], reactive ion etching (RIE) [4], electrochemical etching and metal-assisted chemical etching or metal-catalyzed electroless etching (MCEE) method [5]–[7]. The MCEE method is one of the most favorable methods because of its easily controlled associated parameters, such as cross-sectional shape, diameter, length, and orientation. This method can also be accomplished in a chemical lab with simple and inexpensive equipment. Moreover, there is no apparent limitation on the size and features of SiNWs fabricated using this method, which is easy to scale up in the industry.

Recently, researchers have shown an interest in the development of the SiNWs as a promising candidate for a wide range of applications in solar cells, catalysts, and sensors due to the high surface area of the SiNWs [8]–[11]. The SiNWs/organic semiconductor hybrid solar cells have shown an increase in the power conversion efficiency (PCE) due to the function of the organic layer as a hole-transporting path and the formation of a heterojunction with Si [12]–[14]. Some studies have been carried out on Si nanostructurepoly(3,4-ethylenedioxythiophene) poly(styrene sulfonate) (PEDOT:PSS) hybrid solar cell using nanoparticles [15]–[17]. However, no studies have been found in solar cells application using SiNWs/PEDOT:PSS/gold nanoparticles (AuNPs). AuNPs are known as an important material to enhance photo-carriers in solar cells due to their strong optical field enhancement through localized surface plasmon excitation (LSPR) [18]–[20].

In this work, we used the SiNWs as part of the inorganic semiconductor for hybrid solar cells and PEDOT:PSS as part of the organic semiconductor. To improve the performance of the solar cell, we combined the AuNPs into a hole-transport layer. Finally, the performance of SiNWs/PEDOT:PSS/AuNPs hybrid solar cell with the different concentration ratio of PEDOT:PSS and AuNPs were studied to optimize the SiNWs/PEDOT:PSS/AuNPs hybrid solar cell.

2. Experimental

2.1 SiNW Arrays Fabrication

An n-type Si (100) substrate with a thickness of 525 ± 20 μm and a resistivity of 40–50 Ω·cm were chemically cleaned by using acetone, ethanol, and deionized (DI) water for 10 min in an ultrasonic bath. Then further cleaned with a piranha solution, which is a mixture of H_2SO_4 and H_2O_2 (3:1, v/v), for 20 min and was dried with nitrogen gas. The final cleaning process was done by rinsing the Si wafers with dilute hydrofluoric acid (2% HF) for 2 min to remove the oxide layer on their surface. For the etching process, the SiNW arrays were fabricated by the MCEE method. The concentration of the etching solution was 4.6 M of HF acid and 0.02 M of silver nitrate ($AgNO_3$). The cleaned Si wafers were etched for 5 min and then dipped into DI water to stop the etching reaction. After etching, they were soaked in 50% nitric acid (HNO_3) for 5 min to dissolve the Ag catalyst away from their surfaces. Finally, we cleaned the SiNW arrays with DI water three times and dried with nitrogen gas.

2.2 Device Fabrication

To fabricate SiNWs/PEDOT:PSS/AuNPs hybrid solar cell,

Manuscript received August 7, 2020.
Manuscript revised September 9, 2020.
Manuscript publicized December 8, 2020.

[†]The authors are with Graduate School of Science and Technology and Faculty of Engineering, Niigata University, Niigata-shi, 950–2181 Japan.
[††]The authors are with Department of Physics, Faculty of Science, Chulalongkorn University, 254 Phayathai Road, Pathumwan, Bangkok, 10330 Thailand.
a) E-mail: sukkaneste.t@chula.ac.th
b) E-mail: ababa@eng.niigata-u.ac.jp

DOI: 10.1587/transele.2020OMS0008

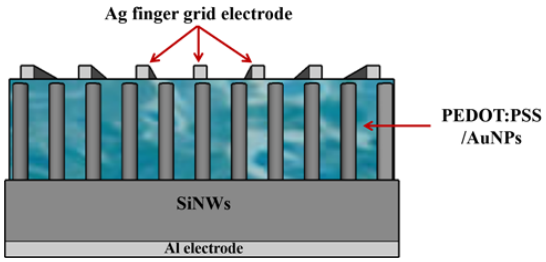

Fig. 1 Schematic diagram of SiNWs/PEDOT:PSS/AuNPs hybrid solar cell.

the SiNW arrays were cleaned with piranha solution for 50 min, followed by cleaning with DI water multiple times. We removed any native oxides from the front and backside of the wafers by immersing them in 2% HF for 2 min. Then, the SiNW arrays were cleaned with DI water and dried with nitrogen gas. Then, the PEDOT:PSS mixed with AuNPs was spin-coated on the surface of the SiNWs at 4000 rpm for 2 min, and then annealed at 140°C for 20 min at room temperature to dry the PEDOT:PSS film. Furthermore, the silver metal finger grid was deposited on the PEDOT:PSS film by vacuum evaporation technique through a shadow mask with an area of 0.46 cm^2 and thickness of 250 nm. Next, aluminum metal was deposited on the cell surface with an area of 1 cm^2 and a thickness of 90 nm. Finally, the devices were annealed at 150°C in a vacuum. The structure of the cell is shown in Fig. 1.

3. Results and Discussions

The morphology of the SiNW/PEDOT:PSS/AuNPs hybrid structure was investigated by scanning electron microscopy (SEM), using a JEOL JEM-6330F field emission electron microscope. Figure 2 shows the cross-sectional image of the SiNW arrays with an average nanowire of length 540 nm and an average diameter of 25 nm. It is noteworthy that the length of nanowires used for the solar cell structures were about the same as the wavelength of the green light. It might be the case that the SiNWs improve the light absorption by light trapping effect [21], [22].

The cross-sectional and top-view SEM images of the SiNWs/PEDOT:PSS are shown in Figs. 3 (a) and 3 (b), respectively. The PEDOT:PSS was spin-coated on the surface of the SiNWs at 4000 rpm for 2 min, followed by annealing at 140°C for 20 min. From Fig. 3 (a), we observed that the average nanowire diameter is 40–50 nm, which is bigger than that of the SiNWs without the deposition of PEDOT:PSS, indicating that the nanowires were covered with PEDOT:PSS. Cross-sectional SEM image in Fig. 3 (b) indicates that the SiNWs arrays are not too condensed and have enough space to deposit the AuNPs not only on the top surface of the SiNWs but also inside the SiNW arrays.

Figure 4 shows the SEM image of the SiNWs/PEDOT:PSS cross-section with AuNPs. It is difficult to confirm the presence of the AuNPs from the image, however, we can observe some roughness or nanoparticle-like structures on

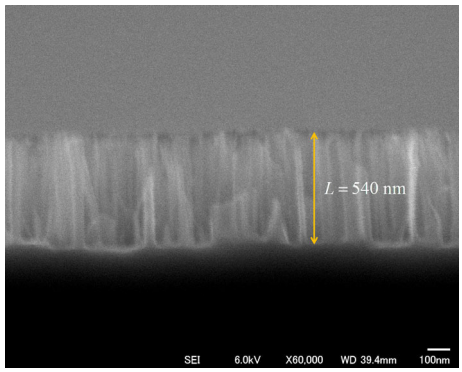

Fig. 2 Cross-sectional scanning electron microscopy (SEM) image of SiNWs with nanowires length of 540 nm.

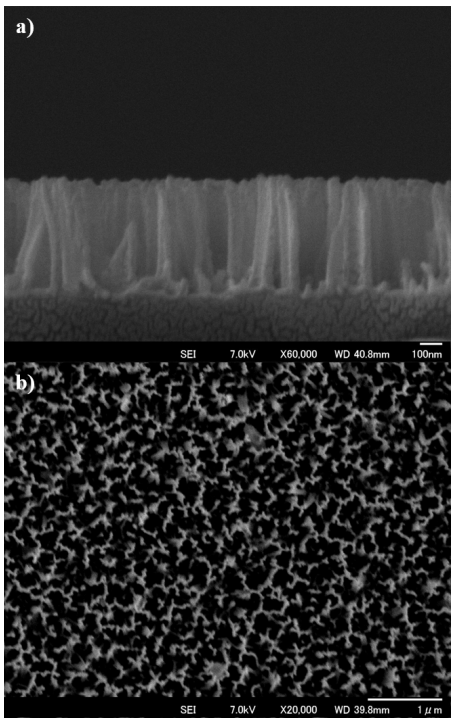

Fig. 3 (a) Cross-sectional and (b) top view of scanning electron microscopy (SEM) images of SiNW arrays coated by PEDOT:PSS.

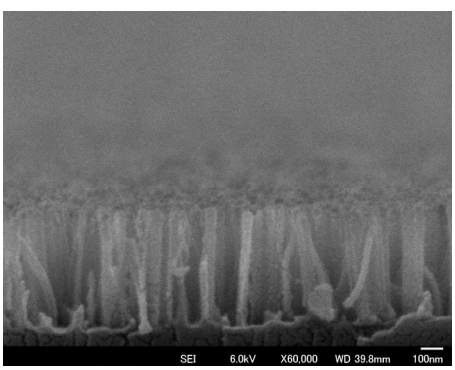

Fig. 4 Cross-sectional scanning electron microscopy (SEM) image of SiNW arrays coated by PEDOT:PSS with AuNPs.

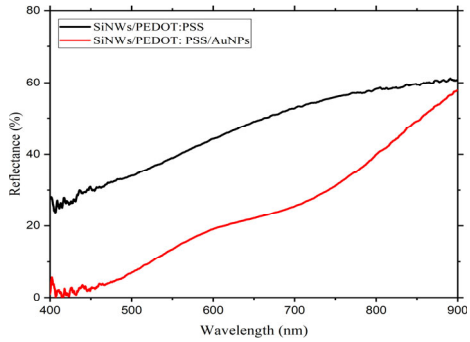

Fig. 5 Reflectance spectra of SiNW arrays coated with PEDOT:PSS only and PEDOT:PSS/AuNPs.

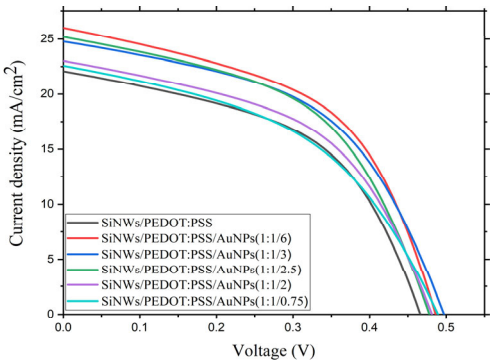

Fig. 6 Current density-voltage (J–V) properties of SiNWs/PEDOT:PSS/AuNPs hybrid solar cell with nanowires length of 540 nm as a function of the concentration rate of PEDOT:PSS and AuNPs.

the top surface and sidewall of the SiNWs. This indicates the penetration of AuNPs into the SiNWs array with PEDOT:PSS and attached to the sidewall of the SiNWs in addition to the deposition on the top surface. This is reasonable because the pore size of the SiNWs array is larger than the diameter of AuNPs (20 nm) as observed in Fig. 3 (b).

To confirm the presence of the AuNPs, we measured reflectance spectra of the SiNWs coated with the PEDOT:PSS mixed with and without AuNPs as shown in Fig. 5. In the reflectance measurements, a white light was irradiated at an incident angle of 5° and the reflected light was detected. The result shows that the reflectance of the SiNWs covered with PEDOT:PSS/AuNPs is lower than that of SiNWs covered with PEDOT:PSS only, indicating the presence of the AuNPs in the system. The enhanced light absorption was due to both light scattering effect and LSPR excitation on the AuNPs. Furthermore, it was noticed that the reflectance of the SiNWs coated with PEDOT:PSS mixed with AuNPs is less than 20% at the wavelength below 600 nm, which corresponds to the wavelength of the LSPR excitation region. This result indicates that the inclusion of AuNPs into the SiNW/PEDOT:PSS can improve the light absorption/optical field in the device [23].

Solar cells consisting of Al/SiNWs/PEDOT:PSS with and without AuNPs were fabricated. The concentration ratio of PEDOT:PSS with AuNPs was varied at the ratios of 1:1/6, 1:1/3, 1:1/2.5, 1:1/2, and 1:1/0.75 to determine the optimum concentration ratio of PEDOT:PSS and AuNPs. The photovoltaic parameters of the cells were measured under AM 1.5G illumination. Figure 6 shows the current density-voltage (J–V) properties of SiNWs/PEDOT:PSS/AuNPs hybrid solar cells with nanowires length of 540 nm as a function of the concentration rate of PEDOT:PSS and AuNPs. The photovoltaic parameters are summarized in Table 1. The solar cell without AuNPs exhibits a short-circuit current density (J_{sc}) value of 22.08 mA/cm^2, open-circuit voltage (V_{oc}) of 0.47 V, fill factor (FF) of 0.50, and a PCE of 6.91%.

From Table 1, the SiNWs/PEDOT:PSS/AuNPs hybrid solar cells show an enhancement of the PCE when the concentration ratio of AuNPs was decreased. The PCE as a function of the concentration of AuNPs is plotted in

Table 1 Photovoltaic parameter of SiNWs/PEDOT:PSS/AuNPs hybrid solar cell as a function of the concentration rate of PEDOT:PSS and AuNPs.

Device	J_{sc} (mA/cm^2)	V_{oc} (V)	FF	PCE (%)
SiNWs/PEDOT:PSS	22.08	0.47	0.50	6.91
SiNWs/PEDOT:PSS/AuNPs (1:1/6)	26.00	0.49	0.51	8.56
SiNWs/PEDOT:PSS/AuNPs (1:1/3)	24.78	0.50	0.50	8.23
SiNWs/PEDOT:PSS/AuNPs (1:1/2.5)	25.20	0.48	0.50	8.03
SiNWs/PEDOT:PSS/AuNPs (1:1/2)	23.02	0.48	0.49	7.30
SiNWs/PEDOT:PSS/AuNPs (1:1/0.75)	22.57	0.49	0.46	6.75

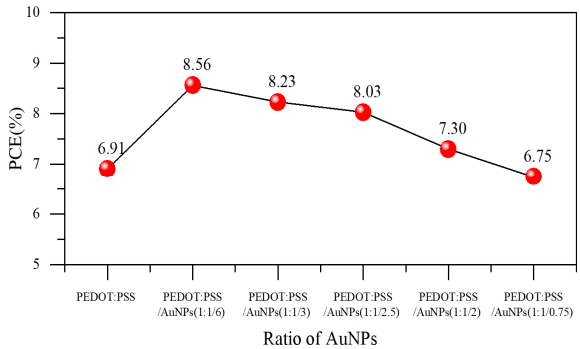

Fig. 7 The power conversion efficiency (PCE) as a function of AuNPs in the SiNWs/PEDOT:PSS/AuNPs solar cells.

Fig. 7. The solar cell with a concentration ratio between PEDOT:PSS and AuNPs of 1:1/6 exhibits the highest performance. The J_{sc}, V_{oc}, FF, and PCE of this cell are 26.00 mA/cm^2, 0.49 V, 0.51, and 8.56%, respectively. The solar cell combined with AuNPs in the hole-transport layer showed an improved J_{sc} of 18% and PCE of 24% compared to the solar cell without AuNPs. The reason that the efficiency decreased at higher ratio than 1:1/6 should be due to too much amount of AuNPs. The loading amount of AuNPs needs to be decided by taken into account the trade-off balance between the effect of strong electric field enhancement in the vicinity of the AuNPs and light transmission in the PEDOT:PSS/AuNPs layer [18]. AuNPs improve the total light absorption at the active layer due to the enhanced electric field at around the AuNPs if the irradiated light sufficiently reaches the active layer. How-

ever, if the amount of AuNPs exceeds an optimum condition, then irradiated light cannot sufficiently pass through the PEDOT:PSS/AuNPs layer, hence the total light absorption in the active layer decreases.

4. Conclusions

The MCEE method was used to fabricate the SiNWs with a nanowire length of 540 nm. The concentration of the etching solution was 4.6 M of HF and 0.02 M of $AgNO_3$ at an etching time of 5 min. The solar cell with AuNPs improved light absorption due to the light scattering and localized surface plasmon excitation. The PCE of the SiNWs/PEDOT:PSS/AuNPs hybrid solar cell increased when the concentration ratio of AuNPs was decreased. We found that the solar cell with the concentration ratio of PEDOT: PSS and AuNPs of 1: 1/6 shows the highest PCE of 8.56%.

Acknowledgments

This work was supported by The 100^{th} Anniversary Chulalongkorn University Fund for Doctoral Scholarship and Japan Society for the Promotion of Science (JSPS) KAKENHI Grant Numbers JP20H02601 and JP17H03231.

References

[1] S.D. Hutagalung, M.M. Fadhali, R.A. Areshi, and F.D. Tan, "Optical and Electrical Characteristics of Silicon Nanowires Prepared by Electroless Etching," Nanoscale Res. Lett., vol.12, no.1, p.425, 2017.

[2] M. Lajvardi, H. Eshghi, M.E. Ghazi, M. Izadifard, and A. Goodarzi, "Structural and optical properties of silicon nanowires synthesized by Ag-assisted chemical etching," Mater. Sci. Semicond. Process., vol.40, pp.556–563, 2015.

[3] F. Demami, L. Ni, R. Rogel, A.C. Salaun, and L. Pichon, "Silicon nanowires synthesis for chemical sensor applications," Procedia Eng., vol.5, pp.351–354, 2010.

[4] M.N.M. Nor, U. Hashim, N.H.A. Halim, N.H.N. Hamat, M. Rusop, R.Y. Subban, N. Kamarulzaman, and W.T. Wui, "Top-Down Approach: Fabrication of Silicon Nanowires using Scanning Electron Microscope based Electron Beam Lithography Method and Inductively Coupled Plasma-Reactive Ion Etching," AIP Conf. Proc., vol.1217, pp.272–278, 2010.

[5] Z. Huang, N. Geyer, P. Werner, J. de Boor, and U. Gosele, "Metal-assisted Chemical Etching of Silicon: A Review," Adv. Mater., vol.23, no.2, pp.285–308, 2011.

[6] L. Liu, K.-Q. Peng, Y. Hu, X.-L. Wu, and S.-T. Lee, "Fabrication of Silicon Nanowire Arrays by Macroscopic Galvanic Cell-Driven Metal Catalyzed Electroless Etching in Aerated HF Solution," Adv. Mater., vol.26, no.9, pp.1410–1413, 2014.

[7] Y. Hu, K.-Q. Peng, Z. Qiao, X. Huang, F.-Q. Zhang, R.-N. Sun, X.-M. Meng, and S.-T. Lee, "Metal-Catalyzed Electroless Etching of Silicon in Aerated HF/H_2O Vapor for Facile Fabrication of Silicon Nanostructures," Nano Lett., vol.14, no.8, pp.4212–4219, 2014.

[8] G.G. Pethuraja, H. Efstathiadis, C. Rouse, M.V. Rane-Fondacaro, A.K. Sood, and P. Haldar, "Silicon Nanowire Development for Solar Cell Devices," 38th IEEE Photovoltaic Spec. Conf., pp.001911–001916, 2012.

[9] Y.M.A. Yamada, Y. Yuyama, T. Sato, S. Fujikawa, and Y. Uozumi, "A Palladium-Nanoparticle and Silicon-Nanowire-Array Hybrid: A Platform for Catalytic Heterogeneous Reactions," Angew. Chem. Int. Ed., vol.53, pp.127–131, 2014.

[10] B. Zhang, J. Jie, X. Zhang, X. Ou, and X. Zhang, "Large-scale fabrication of silicon nanowires for solar energy applications," ACS Appl. Mater. Interfaces, vol.9, no.40, pp.34527–34543, 2017.

[11] P. Namdari, H. Daraee, and A. Eatemadi, "Recent Advances in Silicon Nanowire Biosensors: Synthesis Methods, Properties, and Applications," Nanoscale Res. Lett., vol.11, no.1, p.406, 2016.

[12] K. Sato, M. Dutta, and N. Fukata, "Inorganic/organic hybrid solar cells: Optimal carrier transport in vertically aligned silicon nanowire arrays," Nanoscale, vol.6, no.11, pp.6092–6101, 2014.

[13] T. Subramani, H.-J. Syu, C.-C. Hsueh, C.-T. Liu, T.-C. Linb, and C.-F. Lin, "Optical trapping enhancement from high density silicon nanohole and nanowire arrays for efficient hybrid organic–inorganic solar cells," RSC Adv., vol.5, no.17, pp.13224–13233, 2015.

[14] W. Lu, C. Wang, W. Yue, and L. Chen, "Si/PEDOT:PSS core/shell nanowire arrays for efficient hybrid solar cells," Nanoscale, vol.3, no.9, p.3631, 2011.

[15] T. Subramani, J. Chen, Y.-L. Sun, W. Jevasuwan, and N. Fukata, "High-efficiency silicon hybrid solar cells employing nanocrystalline Si quantum dots and Si nanotips for energy management," Nano Energy, vol.35, pp.154–160, 2017.

[16] H. Wang, J. Wang, L. Hong, Y.H. Tan, C.S. Tan, and Rusli, "Thin Film Silicon Nanowire/PEDOT:PSS Hybrid Solar Cells with Surface Treatment," Nanoscale Res. Lett., vol.11, no.1, p.311, 2016.

[17] R. Lu, L. Xu, Z. Ge, R. Li, J. Xu, L. Yu, and K. Chen, "Improved Efficiency of Silicon Nanoholes/Gold Nanoparticles/Organic Hybrid Solar Cells via Localized Surface Plasmon Resonance," Nanoscale Res. Lett., vol.11, no.1, p.160, 2016.

[18] A. Pangdam, S. Nootchanat, R. Ishikawa, K. Shinbo, K. Kato, F. Kaneko, C. Thammacharoen, S. Ekgasit, and A. Baba, " Effect of urchin-like gold nanoparticles in organic thin-film solar cells," Phys. Chem. Chem. Phys., vol.18, no.27, pp.18500–18506, 2016.

[19] T. Putnin, C. Lertvachirapaiboon, R. Ishikawa, K. Shinbo, K. Kato, S. Ekgasit, K. Ounnunkad, and A. Baba, "Enhanced organic solar cell performance: Multiple surface plasmon resonance and incorporation of silver nanodisks into a grating-structure electrode," Opto-Electronic Adv., vol.2, p.190010, 2019.

[20] S. Phetsang, A. Phengdaam, C. Lertvachirapaiboon, R. Ishikawa, K. Shinbo, K. Kato, P. Mungkornasawakul, K. Ounnunkad, and A. Baba, "Investigation of a gold quantum dot/plasmonic gold nanoparticle system for improvement of organic solar cells," Nanoscale Adv., vol.1, no.2, pp.792–798, 2019.

[21] E. Garnett and P. Yang, "Light Trapping in Silicon Nanowire Solar Cells," Nano Lett., vol.10, no.3, pp.1082–1087, 2010.

[22] W. Ding, R. Jia, H. Li, C. Chen, Y. Sun, Z. Jin, and X. Liu, "Design of two dimensional silicon nanowire arrays for antireflection and light trapping in silicon solar cells," J. Appl. Phys., vol.115, no.1, p.014307, 2014.

[23] N. Chander, A.F. Khan, E. Thouti, S.K. Sardana, P.S. Chandrasekhar, V. Dutta, and V.K. Komaral, "Size and concentration effects of gold nanoparticles on optical and electrical properties of plasmonic dye sensitized solar cells," Solar Energy, vol.10, pp.11–23, 2014.